Noise contribution to the correlation between temperature-induced localized reflectance of diabetic skin and blood glucose

Michael G. Lowery
Brenda Calfin
Shu-jen Yeh
Tao Doan
Eric Shain
Charles Hanna
Ronald Hohs
Stan Kantor
John Lindberg
Omar S. Khalil
Abbott Laboratories
100 Abbott Park Road
Abbott Park, Illinois 60064

Abstract. We used the effect of temperature on the localized reflectance of human skin to assess the role of noise sources on the correlation between temperature-induced fractional change in optical density of human skin (ΔOD_T) and blood glucose concentration [BG]. Two temperature-controlled optical probes at 30°C contacted the skin, one was then cooled by −10°C; the other was heated by +10°C. ΔOD_T upon cooling or heating was correlated with capillary [BG] of diabetic volunteers over a period of three days. Calibration models in the first two days were used to predict [BG] in the third day. We examined the conditions where the correlation coefficient (R^2) for predicting [BG] in a third day ranked higher than R^2 values resulting from fitting permutations of randomized [BG] to the same ΔOD_T values. It was possible to establish a four-term linear regression correlation between ΔOD_T upon cooling and [BG] with a correlation coefficient higher than that of an established noise threshold in diabetic patients that were mostly females with less than 20 years of diabetes duration. The ability to predict [BG] values with a correlation coefficient above biological and body-interface noise varied between the cases of cooling and heating. [DOI: 10.1117/1.2360529]

Keywords: localized reflectance; temperature-induced fractional change in optical density; human skin; blood glucose concentration; biological noise; repositioning noise.

Paper 05360R received Dec. 2, 2005; revised manuscript received Jun. 2, 2006; accepted for publication Jun. 8, 2006; published online Oct. 10, 2006.

1 Introduction

Noninvasive (NI) measurements of glucose in the human body have been of considerable interest in the past decade.[1,2] Near infrared (NIR) transmittance measurements track weak glucose absorption features expressed by its absorption coefficient μ_a.[3–6] Scattering measurements track glucose effect on tissue scattering coefficient, μ_s'.[7,8] The optical signals are extremely weak and can be masked by biological and body-interface noise. The ability of a NI method to determine glucose depends on the ability of the measured variables to correlate with blood glucose concentration [BG] values with a correlation coefficient that ranks higher than correlation coefficients obtained from regression of the same optical signals and sets of random numbers.

There is a dearth of information on the noise sources in a NI glucose measurement. Body-interface noise includes probe-repositioning error with respect to skin, change in skin properties due to environmental temperature and humidity, circadian changes in cutaneous circulation, and sweating due to long contact between skin and the measuring probe. Errors due to probe repositioning with respect to the skin were identified as a noise source, and a fixture to minimize them was proposed.[9] The role of biological and structural effects of skin as noise sources has not been adequately explored. NI optical measurements are mostly performed through the skin. Transcutaneous NI glucose optical methods considered human skin as a passive translucent optical window, like any other cuvette window, through which the optical measurement is performed. Skin properties were found to depend on diabetes,[10–13] on gender,[14] and on application of external stimuli.[15] Interaction between a measuring probe and skin involves heat transfer from the probe to the skin and vice versa. NIR optical properties of human skin vary with temperature,[16–18] and skin thermo-optical response to test the diabetic state and track glucose concentration changes,[17,18] which presented an impetus for this work.

We used localized reflectance measurements to study changes in optical density, ΔOD_T (logarithm of the ratio of localized reflectance at two temperatures) of dorsal side forearm skin upon changing skin temperature. ΔOD_T incorporates temperature effects on both μ_a and μ_s'. Increase in [BG] or lowering of temperature decreases μ_s'. Increase in either [BG] or temperature increases blood perfusion and hence μ_a (see Ref. 1 for a review). Change in temperature and/or [BG] af-

Address all correspondence to Omar S. Khalil, Pharos Biomedical Research, 195 N. Harbor Dr., Unit 4806, Chicago, IL 60601; Tel.: (312) 938-0865; E-mail: Omar.Khalil@pharosbiomed.com

1083-3668/2006/11(5)/054029/8/$22.00 © 2006 SPIE

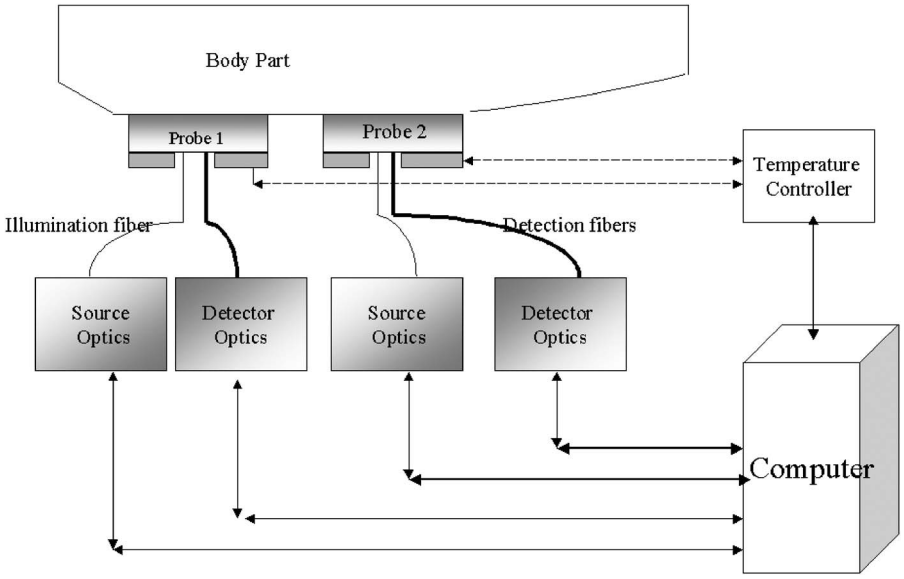

Fig. 1 Schematic of the dual probe system.

fect both of μ_a and of μ_s', which suggests a possible correlation between [BG] and ΔOD_T.

The purpose of this work is to answer two questions. The first: Can we use temperature-induced change in localized reflectance (ΔOD_T) of human skin to segregate glucose-related signals from noise. The second question: Does skin play the role of a mere optical window for NI determination of [BG] or it is an active component contributing to the measurement noise because of the effect of diabetes and glucose on its properties.

2 Materials and Methods

2.1 *Instrument*

We constructed an instrument to measure the temperature-dependence of tissue localized reflectance. It comprised two identical independently temperature-controlled probes mounted on a common fixture and brought in touch with the forearm. Figure 1 shows a schematic diagram of the optical system. Figure 2 shows the details of an optical probe. Each optical probe had a light source module, a human interface module, and a signal detection module that are interconnected through a branched fiber bundle.

The light source module had four light emitting diodes (LEDs) mounted into a circular disk (a), each LED plastic cap was machined to a flat end and was placed in touch with the end of one of four fibers (b), each was a 400-μm diameter silica fiber. Light from the end ferrule passed through a 7-mm aperture and was focused onto the input end of the illuminating fiber (g), using lens system (c), which is a combination of two achromats. Part of the light was diverted by a beamsplitter (d) and focused onto a reference silicon photodiode (e) and amplifier (f) to correct for LEDs intensity fluctuations. Four drive circuits modulated the LEDs.

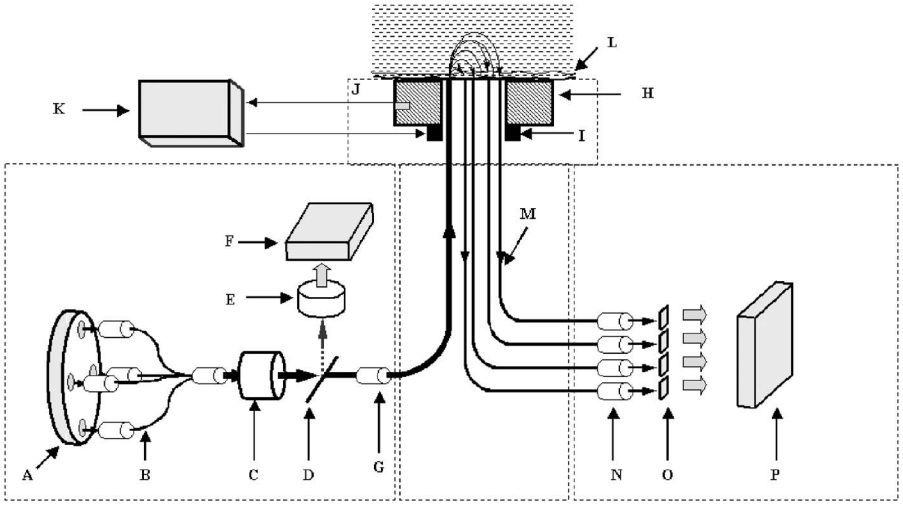

Fig. 2 Detailed schematic of a single optical probe showing the illumination, detection, and body-interface elements and optical components.

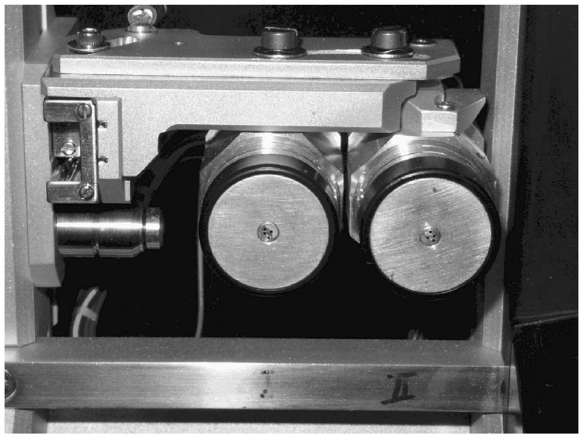

Fig. 3 A photo of the two temperature-controlled localized reflectance probes mounted in the body interface. The outer black ring is an insulating Delrin™ ring. The large metallic inner disk is a 2-cm diameter aluminum disk with the thermoelectric element glued to its back. At the center is a ferrule of the fiber optic bundle having the illumination fiber and the detection fibers.

Each probe had a common tip at the center of a 2-cm diameter aluminum disk (h) glued to a thermoelectric element (i) (Marlow Industries, Dallas, Texas). A T-type thermocouple (j) embedded in the disk provided feedback to the temperature controller (k) (Marlow Industries). The disk touched skin surface (l). Reemitted light was collected by four detection fibers (m), which ended in detection tip (n), and were imaged onto a photodiode (PD) (o). The signal from each PD was separately amplified by (p) and routed to the analog-to-digital boards in the personal computer chassis. The wavelengths and modulation frequency of each of the LEDs were 590 nm at 819 Hz, 660 nm at 1024 Hz, 890 nm at 455 Hz, and 935 nm at 585 Hz. The half-bandwidth of the LEDs was 25, 25, 50, and 50 nm, respectively. The illumination power for each fiber was 1.4 to 5.0 μW. The wavelengths were in the hemoglobin absorption bands. The 660- and 935-nm LEDs approximate wavelengths used in measurements of blood oxygen saturation. None of these wavelengths corresponds to glucose absorption. The signals detected are predominantly due to light scattering by cutaneous structural components and light absorption by blood hemoglobin.

Distances between the source fiber and the light collecting fibers, source-detector (S-D) distances (r), were 0.44, 0.90, 1.21, and 1.84 mm, respectively. We selected the S-D distances to limit collected light to within a 2-mm sampling depth, where temperature can be easily varied and controlled independent of the body core temperature.[16–18] The signal from each detector corresponded to one S-D distance (r), and the signal at each modulation frequency corresponded to one λ. Signals were collected every 5 s. The optical probes shown in Fig. 3 touched the dorsal side of the forearm at a constant force of $\approx$45 g/cm^2. A LABVIEW™ program controlled instrument functions, thermal management, and data acquisition.

2.2 *Subjects*

The study was conducted at Abbott Clinical Pharmacology Research Unit, Victory Memorial Hospital (Waukegan, Illinois), using a protocol approved by the hospital institutional review board. Twenty diabetic volunteers on insulin treatment and within the age range of 18 to 65 years were recruited and signed informed consent forms. Fifteen of them had multiple comorbidities and diabetes complications. Volunteers had insulin injections, oral diabetes medications, and other prescribed medications during a three-day confinement and were served meals with known caloric-content depending on their weight. Those $<$130 pounds had 1800 kcal in the first day and 2000 kcal in the other days, and those $>$130 pounds had 2000 kcal in the first day and 2500 kcal in days 2 and 3. The caloric intake was varied over the course of the study to provide ranges of glucose concentration for the calibration set. The first day had the lowest caloric content to ensure that patient's [BG] values did not substantially increase above their usual range. Ten reference [BG] values per day were determined using a home glucose meter (Bayer Elite^R, Bayer Corporation, Elkhart, Indiana). Its accuracy was $<$10%.

The probes temperature was raised to 30°C at the start of the experiment. We applied a thin layer of silicon oil to an area on the dorsal side of the left arm to enhance heat transfer. The subject sat in a chair and with the left arm in the body-interface cradle, retracted the spring-loaded dual probe with the right hand and started a countdown. At count zero, the subject released the probe toward the skin as the operator clicked the start-run icon. The probes were maintained at 30°C for 30 s, temperature was then ramped at a rate of -3.33 or $+3.33$°C·min^{-1} for 180 s, leading to a -10°C change of the cooling probe and a $+10$°C change of the heating probe. The temperature of each probe was then returned to 30°C and maintained at this final temperature for 30 s. Data collection time was 240 s. Probe temperatures and measurement duration times were selected based on a test for maximum comfort on a set of volunteers. The upper and lower temperature limits ensured that skin redness for fair-skinned volunteers disappeared in less than 5 min of end of the measurement.

3 Results

3.1 *Signal Output*

We identified data sets that had sudden changes in the optical signals caused by the movement of the forearm relative to the probes (motion artifacts) by running an exponential moving point average on the stream of data points. Data sets that showed changes in the signal magnitude higher than a set threshold were rejected.[19]

Figure 4 shows examples for the outputs of the cooling probe and the heating probe expressed as $2.303\log(R_t/R_{30\ s})$ for the first run on the first patient at the 0.44 mm S-D distance. Signals were normalized to the 30-s time point, that is at a 30°C temperature point. The signal changed at $\approx$210 s when both probes were brought back to 30°C.

3.2 *Data Analysis*

Signals were collected at each λ, r, and probe temperature T, as the localized reflectance, $\mathcal{R}(\lambda_i, r_j, T)$. The natural logarithm of the ratio of the signals at two temperatures was calculated for each probe as $\ln[\mathcal{R}(\lambda_i, r_j, T_2)/\mathcal{R}(\lambda_i, r_j, T_1)]$, T_1 and T_2 are the probe temperatures at the start and end of temperature ramping. Since the change in temperature induces

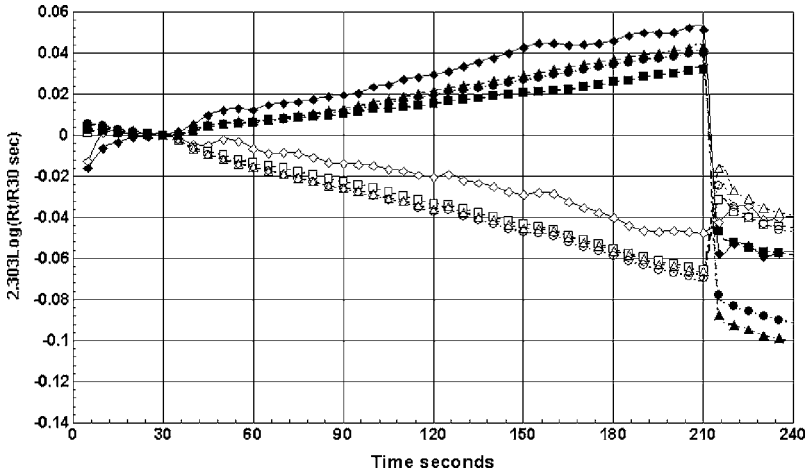

Fig. 4 Time series of the output of the cooling and heating localized reflectance probe at 0.44-mm S-D distance and at the four wavelengths. Open symbols are for the cooling probe and solid symbols for the heating probe ◇ 590 nm, □ 660 nm, ◦ 890 nm, and △ 935 nm.

a small change in $\mathcal{R}$ using the expansion $\ln(1+x)=x+x^2/2!+x^3/3!+\cdots\approx x$, when $x\ll 1$, leads to Eq. (1)

$$\ln[\mathcal{R}(\lambda_i,r_j,\mathrm{T}_2)/\mathcal{R}(\lambda_i,r_j,\mathrm{T}_1)]=\ln(1+\Delta\mathcal{R}_\mathrm{T})=\Delta\mathcal{R}_\mathrm{T}. \quad (1)$$

$\Delta\mathcal{R}_T$ is the temperature-induced change in $\mathcal{R}(\lambda_i,r_j)$ and can be expressed in optical density terms as $\Delta\mathrm{OD}_T$, cooling-induced change, $\Delta\mathrm{OD}_{TC}$, and heating-induced change, $\Delta\mathrm{OD}_{TH}$, leading to

$$2.303\log_{10}[\mathcal{R}(\lambda_i,r_j,\mathrm{T}_2)/\mathcal{R}(\lambda_i,r_j,\mathrm{T}_1)]=2.303\Delta\mathcal{R}_\mathrm{T}=-\Delta\mathrm{OD}_\mathrm{T}(\lambda_i,r_j), \quad (2)$$

$$2.303\log_{10}[\mathcal{R}(\lambda_i,r_j,\mathrm{T}_2)/\mathcal{R}(\lambda_i,r_j,\mathrm{T}_1)]\ \text{cooling}=2.303\Delta\mathcal{R}_\mathrm{TC}=-\Delta\mathrm{OD}_\mathrm{TC}(\lambda_i,r_j), \quad (3)$$

$$2.303\log_{10}[\mathcal{R}(\lambda_i,r_j,\mathrm{T}_2)/\mathcal{R}(\lambda_i,r_j,\mathrm{T}_1)]\ \text{heating}=2.303\Delta\mathcal{R}_\mathrm{TH}=-\Delta\mathrm{OD}_\mathrm{TH}(\lambda_i,r_j). \quad (4)$$

There is a minus sign for $\Delta\mathrm{OD}_T(\lambda_i,r_j)$ because the reflected light intensity varies in the opposite direction to change in optical density, that is, opposite to the light absorbed. Figures 5(a)–5(d) display examples of combined plots of $\Delta\mathrm{OD}_{TC}(\lambda_i,r_j)$ and $\Delta\mathrm{OD}_{TH}(\lambda_i,r_j)$ as expressed by Eqs. (3) and (4) plotted as a function of temperature. $\Delta\mathrm{OD}_{TC}$ response is depicted by traces in the 20 °C to 30 °C temperature range, and $\Delta\mathrm{OD}_{TH}$ response is depicted by traces in the 30 to 40 °C temperature range of the plots of Figs. 5(a)–5(d). The traces in Fig. 5(a) show increase in reflected light intensity ($-\Delta\mathrm{OD}_T$) with increasing temperature, indicating the prevalence of scattering at the 0.44-mm S-D distance. The S-D distance increases, and the change in reflected light intensity with temperature decreases, that is, OD increases and reaches a maximum at 1.84-mm S-D distance for the heating probe due to increased blood perfusion, as shown in Fig. 5(d). Light sampled at the longer S-D distance is reflected from deeper cutaneous layers. The cooling probe causes light penetration to deeper layers whereby the light beam samples the deeper vascular structures.[16]

We tested the correlation between [BG] and either or both of $\Delta\mathrm{OD}_{TC}$ and $\Delta\mathrm{OD}_{TH}$ using the four-term linear regression Eqs. (5) and (6)

$$[\mathrm{BG}]=\mathrm{a}_0+\sum\nolimits_\mathrm{n}\mathrm{a}_\mathrm{n}\Delta\mathcal{R}_\mathrm{TC}(\lambda_\mathrm{i},r_\mathrm{j})_\mathrm{n}=\mathrm{c}_0+\sum\nolimits_\mathrm{n}\mathrm{c}_\mathrm{n}\Delta\mathrm{OD}_\mathrm{TC}, \quad (5)$$

$$[\mathrm{BG}]=\mathrm{b}_0+\sum\nolimits_\mathrm{n}\mathrm{b}_\mathrm{n}\Delta\mathcal{R}_\mathrm{TH}(\lambda_\mathrm{i},r_\mathrm{j})_\mathrm{n}=\mathrm{d}_0+\sum\nolimits_\mathrm{n}\mathrm{d}_\mathrm{n}\Delta\mathrm{OD}_\mathrm{TH}. \quad (6)$$

We determined $\Delta\mathrm{OD}_{TC}(\lambda_i,r_j)$ and $\Delta\mathrm{OD}_{TH}(\lambda_i,r_j)$ from $(\mathcal{R}_{20°\mathrm{C}}/\mathcal{R}_{30°\mathrm{C}})$ and $(\mathcal{R}_{40°\mathrm{C}}/\mathcal{R}_{30°\mathrm{C}})$ and were fitted to [BG] values using Eqs. (5) and (6). We calculated the set of coefficients c_0, d_0, c_n, and d_n for each possible combination of $\Delta\mathrm{OD}_{TC}$ and $\Delta\mathrm{OD}_{TH}$ to provide a least-squares fit to [BG]. We used 16 λ_i/r_j combinations in the regression analysis, leading to a total of 1820 possible four-variable combinations for a single probe, and 32 λ_i/r_j variables or 35 960 possible four-variable combinations using the output of both probes. We selected the regression model having the lowest standard error of predicting [BG] in day 3 (see Table 1). We designed a statistical test to rank the likelihood of a true correlation of $\Delta\mathrm{OD}_T$ with [BG] rather than with random noise.

We calculated the model's correlation coefficient (R^2) in day 3 and ranked its magnitude against the model's R^2 values that were similarly calculated using randomized [BG] values and the experimentally determined $\Delta\mathrm{OD}_T$ data in day 3. We performed the calculation separately for each volunteer and used the results to assess the contribution of random noise to the correlation between $\Delta\mathrm{OD}_T$ and [BG].

We established a noise threshold above which we considered that a [BG] prediction is valid by generating 499 random sequences of reference [BG] values in day 3 for each volunteer and correlating these sets with $\Delta\mathrm{OD}_T$ values. We as-

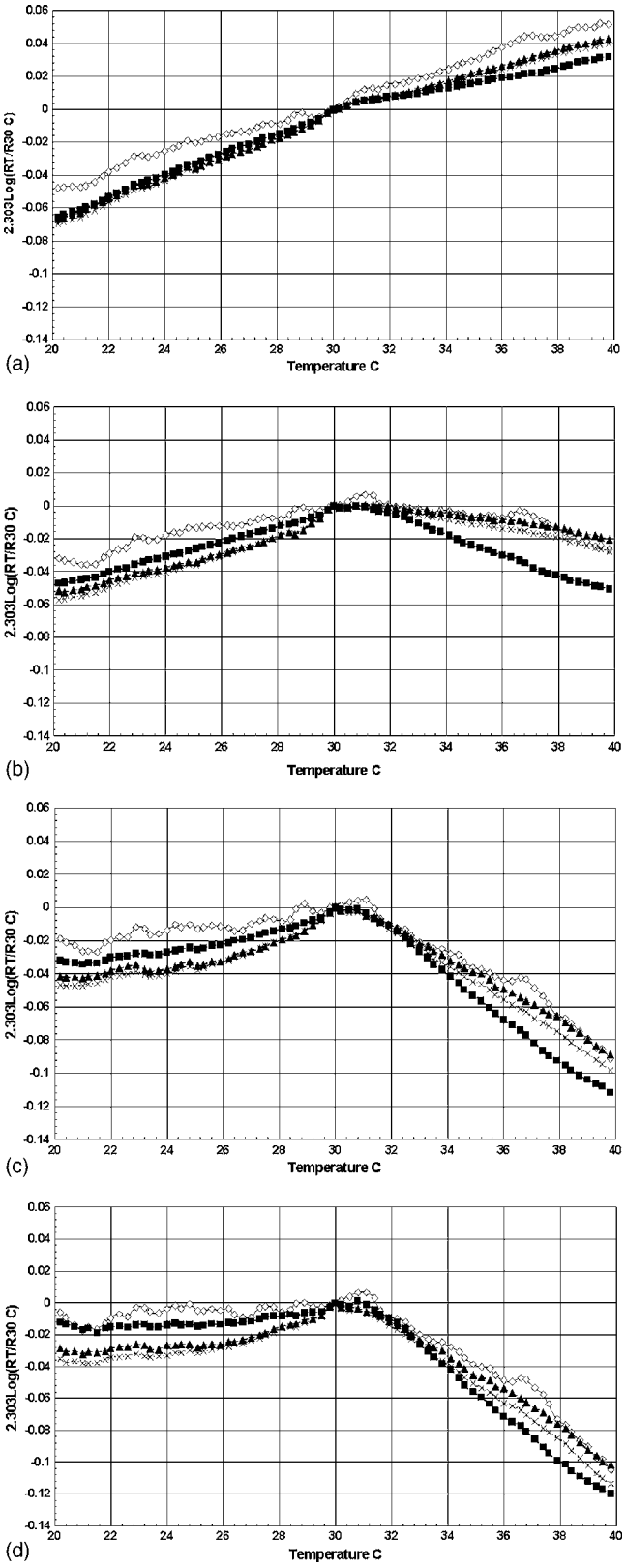

Fig. 5 Plots of the change in ΔOD_T as a function of temperature for the two probes various S-D distances at wavelengths (a) D =0.44 mm: ◇ 590 nm, ■ 660 nm, X 890 nm, and ▲ 935 nm; (b) D=0.90 mm: ◇ 590 nm, ■ 660 nm, X 890 nm, and ▲ 935 nm; (c) D=0.1.21 mm: ◇ 590 nm, ■ 660 nm, X 890 nm, and ▲ 935 nm; (d) D=1.84 mm: ◇ 590 nm, ■ 660 nm, X 890 nm, and ▲ 935 nm.

Table 1 Results of four-variable linear model prediction of third-day [BG] values. (*) designates the rank of R^2 for the correlation with glucose concentration with respect to the R^2 values obtained by fitting 499 permutations of randomized day 3 glucose data to the optical signals. Values in bold lettering ranked above the set noise thresholds.

Probes		Cooling probe		Heating probe		Both probes	
Number of variables		16		16		32	
Volunteer	Runs, day 3	R^2	Rank*	R^2	Rank*	R^2	Rank*
AMP	10	**0.575**	**84**%	0.266	42%	0.512	40%
GRR	8	**0.671**	**78**%	0.107	23%	0.564	42%
DSG	11	0.080	18%	0.024	9%	0.080	2%
A-D	10	0.055	29%	0.028	18%	0.088	16%
JMS	11	**0.492**	**95**%	**0.527**	**90**%	**0.801**	**99**%
S-H	11	**0.405**	**78**%	0.297	37%	**0.578**	**72**%
GED	10	**0.570**	**86**%	0.278	29%	0.597	67%
MTM	10	0.183	40%	0.402	63%	0.529	44%
WSM	10	0.214	56%	0.222	49%	0.338	47%
CND	9	0.145	32%	0.025	4%	0.575	68%
JLT	10	**0.314**	**71**%	0.245	64%	**0.606**	**89**%
PJV	8	**0.425**	**79**%	**0.604**	**90**%	**0.538**	**83**%
JES	9	0.445	48%	0.023	9%	0.510	30%
CRK	8	0.098	20%	0.599	69%	0.587	38%
CJK	8	**0.637**	**78**%	.198	20%	0.637	52%

sumed these random permutations to mimic the sum of body-interface noise and physiological noise. We applied the regression model to predict glucose values for each random permutation and to identify a new optimum set of ΔOD_T, which we used to recalculate the R^2 value for day 3. This process yielded 499 new R^2 values for each patient to compare with the R^2 value corresponding to the correct sequence of [BG] in day 3. We considered a volunteer to exhibit a valid correlation between [BG] and ΔOD_T if the R^2 value for true glucose correlation ranked higher in magnitude than arbitrary threshold of 70% of the 499 new R^2 values generated using randomized [BG] data (see Table 2). We considered a ranking less than the 70% threshold to indicate that biological and body-interface noise dominated ΔOD_T data and produced a correlation with [BG] that was comparable to results from pure random chance correlation.

3.3 *Linear Regression Results*

Using the 16-variable ΔOD_{TC} resulted in 8 of 15 patients (53%) having an R^2 that ranked above the 70% threshold. There was a stronger correlation between [BG] and ΔOD_{TC}

Table 2 Volunteer characteristics and correlation parameters for ΔOD_{TC} versus [BG]. (*) designates the rank of R^2 for the correlation with glucose concentration with respect to the R^2 values obtained by fitting 499 permutations of randomized day 3 glucose data to the optical signals. Values in bold lettering ranked above the set noise thresholds.

Volunteer	Gender	Type of diabetes	Age	Years with diabetes	R^2	Rank*
AMP	F	1	33	13	**0.575**	**84**%
GRR	M	2	62	16	**0.671**	**78**%
DSG	M	1	57	39	0.080	18%
A-D	F	2	44	15	0.055	29%
JMS	F	2	44	7	**0.492**	**95**%
S-H	F	1	38	14	**0.405**	**78**%
GED	F	2	47	5	**0.570**	**86**%
MTM	M	2	66	22	0.183	40%
WSM	M	1	41	20	0.214	56%
CND	M	2	61	20	0.145	32%
JLT	M	2	62	2	**0.314**	**71**%
PJV	M	1	49	29	**0.425**	**79**%
JES	M	2	61	20	0.445	48%
CRK	M	1	19	12	0.098	20%
CJK	F	2	59	8	**0.637**	**78**%

(53%) rather than between [BG] and ΔOD_{TH} (13%), or the combined ΔOD_{TC} and ΔOD_{TH} (27%). We calculated the dependence of $d(\Delta OD_{TC})/dT$ and $d(\Delta OD_{TH})/dT$ on the S-D distance, which represents in different cutaneous depths. Figures 6(a) and 6(b) show these plots. The cooling response curves showed systematic decrease in $d(\Delta OD_{TC})/dT$ with S-D distance. The response was nearly linear with S-D distance for the cooling probe. The slope $d(\Delta OD_{TH})/dT$ showed a linear steep decrease up to a distance of 1.21 mm, an inflection point at 1.21 mm, and then flattened between 1.21- and 1.84-mm S-D distances. The temperature effect on the scattering coefficient is linear and reversible.[16] This difference in $d(\Delta OD_{TC})/dT$ and $d(\Delta OD_{TH})/dT$ suggests that the vascular response to heating differs from that due to cooling. It is difficult to establish if this is one of the sources of loss of correlation between ΔOD_{TH} (heating) and [BG].

We tested the dependence ability to correlate ΔOD_{TC} and [BG] above the noise threshold with the age of the volunteer, mean body mass index, %HbA1c, gender, and duration of diabetes as summarized in Table 3. There was considerable overlap among patient data, except for the presence of two distinct groups, one with diabetes duration <20 years (mean=11.1±4.2) and another with diabetes duration >20 years (mean=24.3±7.3). Six of the eight volunteers with R^2 above the noise threshold (75%) had diabetes duration <20 years. Five of these six patients (62%) were females. One female patient had diabetes duration <20 years, but R^2 for her data set was lower than that of the noise threshold.

Table 3 Summary of clinical data

	Duration of diabetes	
Parameters	<20 years	>20 years
Number of volunteers (total 15)	8	7
Mean age (years)	43.3±13.8	55±8.2
Duration of diabetes (years)	11.1±4.2	24.3±7.3
Body mass index	30.4±7.3	28.5±2.9
%HbA1c	7.2±1.1	6.8±0.9
Number of females	6	0
Number of males	2	7
Number (percent) of volunteers with R^2 ranking above noise ceiling	6 (75%)	2 (29%)
Number (percent) of volunteers with R^2 ranking below noise ceiling	2 (25%)	5 (71%)

The wavelengths used in this study (590 to 935 nm) fall within the hemoglobin absorption spectrum. The observations are not due to light absorption by glucose molecules, but due to cutaneous light scattering and light absorption by hemoglobin molecules, that is, cutaneous structural and vascular response. Skin as an optical window changes its properties due to diabetes. These include skin thickness at the extremities and collagen structure.[10–13] Skin thickness also varies with gender.[14] Diabetes affects the response of the cutaneous vascular system to temperature and pressure changes[15,20,21] and affects skin structural properties.[22,23] This, in turn, affects its optical parameters and heat transmission between the probe and the skin, and hence the effect of the transmitted heat on cutaneous structural and vascular properties. Females have thinner cutaneous layers and thicker subcutaneous fat layers than males.[14] Variation in skin thickness by gender and diabetes duration may have caused this subpopulation result reported here. Extending these arguments (in Refs. 10–15 and 20–23) to the results of the present study, females with short diabetes duration have thinner cutaneous layers than males with longer diabetes duration, which may have led to a correlation between ΔOD_{TC} and [BG]. The heating temperature perturbation program may have introduced more noise into the measurement, probably due to sweating or to the erratic opening of capillary shunts as the skin temperature was raised.

4 Conclusions

Skin is not a passive optical window for NI determination of [BG]. It is an active component contributing to the measurement noise because of the effect of diabetes, gender, and glucose on its properties. Variation in skin thickness, due to gender difference and/or diabetes duration, is a potential noise

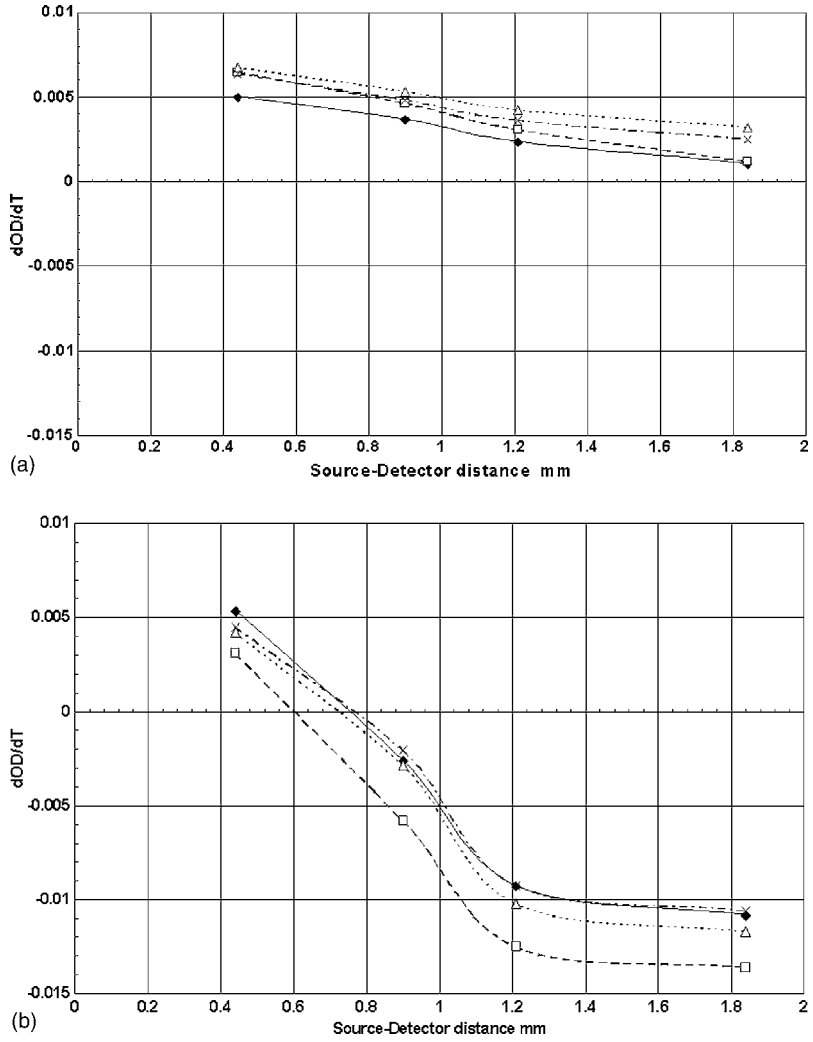

Fig. 6 Plot of the dependence of $d(\Delta OD)/dT$ as a function of the S-D distance: (a) $d(\Delta OD_{TC})/dT$ ◇ for 0.44 mm, ■ for 0.90 mm, X for 1.21 mm, and ▲ for 1.84 mm; (b) $d(\Delta OD_{TC})/dT$ ◇ for 0.44 mm, ■ for 0.90 mm, X for 1.21 mm, and ▲ for 1.84 mm.

source in NI glucose correlation with the thermo-optical response of human skin. Cooling-induced change in localized reflectance from 30 to 20°C, at a temperature ramping rate of $-3.3\,^{\circ}\mathrm{C}\cdot\mathrm{min}^{-1}$, allowed establishing regression equations for predicting [BG] with R^2 ranking above a set noise threshold for diabetic patients that are mostly females with less than 20 years of diabetes duration. Heating the skin from 30 to 40°C at the same ramping rate introduced more noise.

Acknowledgments

The authors acknowledge the help of the members of the Clinical Pharmacology Unit, Global Pharmaceutical Research and Development of Abbott Laboratories in conducting the human experiment and collecting the data.

References

1. O. S. Khalil, "Non-invasive glucose measurement technologies: An update from 1999 to the dawn of the new millennium," *Diabetes Technol. Ther.* **6**, 660–697 (2004).
2. O. S. Khalil, "Spectroscopic and clinical aspects of noninvasive glucose measurements," *Clin. Chem.* **45**, 165–177 (1999).
3. M. R. Robinson, R. P. Eaton, D. M. Haaland, G. W. Keep, E. V. Thomas, B. R. Stalled, and P. L. Robinson, "Noninvasive glucose monitoring in diabetic patients: A preliminary evaluation," *Clin. Chem.* **38**, 1618–1622 (1992).
4. A. Samann, C. F. Fischbacher, K. U. Jagemann, K. Danzer, J. Schuler, L. Papenkordt, and U. A. Muller, "Non-invasive blood glucose monitoring by means of near infrared spectroscopy: Investigation of long-term accuracy and stability," *Exp. Clin. Endocrinol. Diabetes* **108**, 406–413 (2000).
5. K. Maruo, M. Tsurugi, M. Tamura, and Y. Ozaki, "In vivo noninvasive measurement of blood glucose by near-infrared diffuse-reflectance spectroscopy," *Appl. Spectrosc.* **57**, 1236–1244 (2003).
6. A. K. Amerov, J. Chen, and M. A. Arnold, "Molar absorptivities of glucose and other biological molecules in aqueous solutions over the first overtone and combination regions of the near-infrared spectrum," *Appl. Spectrosc.* **58**, 1195–1204 (2004).
7. L. Heinmann et al., "Noninvasive glucose measurements by monitoring of scattering coefficient during oral glucose tolerance tests," *Diabetes Technol. Ther.* **2**, 211–220 (2000).
8. K. V. Larin, M. S. Eledrisi, M. Motamedi, and R. O. Esenaliev, "Noninvasive blood glucose monitoring with optical coherence tomography: A pilot study in human subjects," *Diabetes Care* **25**, 2263–2267 (2002).
9. T. B. Blank, G. Acosta, M. Mattu, M. Makarewicz, S. L. Monfre, A. D. Lorenz, T. L. Ruchti, K. H. Hazen, D. D. Berry, and R. E. Abul-Haj, Inventors, "Optical sampling interface system for *in-vivo* measurement of tissue," U.S. Patent Application Publication US 2005/0203359 A1 (2005).

10. C. Arhtur and R. M. Huntly, "Quantitative determination of skin thickness in diabetes mellitus. Relationship to disease parameters," *J. Med.* **21**, 257–264 (1990).
11. A. Collier, A. W. Patrick, D. Bell, D. M. Matthews, C. C. A. McIntyre, D. J. Ewing, and B. F. Clarke, "Relationship of skin thickness to duration of diabetes, glycemic control and diabetes complications in male IDDM patients," *Diabetes Care* **12**, 309–312 (1989).
12. R. A. Malik, J. Metcalfe, A. K. Sharma, J. L. Day, and G. Rayman, "Skin epidermal thickness and vascular density in type 1 Diabetes," *Diabetes Med.* **9**, 263–267 (1992).
13. T. Forst, P. Kaan, A. Pfutzner, R. Lobmann, T. Schafer, and J. Beyer, "Association between 'diabetic thick skin syndrome' and neurological disorders in diabetes mellitus," *Acta Diabetol* **31**, 73–77 (1994).
14. S. Shuster, M. M. Black, and E. McVitie, "The influence of age and sex on skin thickness, skin collagen and density," *Br. J. Dermatol.* **93**, 639–643 (1975).
15. G. Rayman, S. A. Williams, P. D. Spenser, L. H. Smajie, P. H. Wise, and J. E. Tooke, "Impaired microvascular hyperemic response to minor skin trauma in type 1 diabetes," *Br. Med. J.* **292**, 1295–1298 (1986).
16. O. S. Khalil, S.-J. Yeh, M. G. Lowery, X. Wu, C. F. Hanna, S. Kantor, T.-W. Jeng, J. Kanger, R. A. Bolt, and F. F. de Mul, "Temperature modulation of optical properties of human skin," *J. Biomed. Opt.* **8**, 191–205 (2003).
17. S.-J. Yeh, O. S. Khalil, C. F. Hanna, and S. Kantor, "Near infrared thermo-optical response of the localized reflectance of intact diabetic and non-diabetic human skin," *J. Biomed. Opt.* **8**, 534–544 (2003).
18. S.-J. Yeh, C. F. Hanna, and O. S. Khalil, "Tracking blood glucose changes in cutaneous tissue by temperature-modulated localized reflectance measurements," *Clin. Chem.* **49**, 924–934 (2003).
19. M. G. Lowery, E. B. Shain, and O. S. Khalil, Inventors, "Method for detecting artifacts in data," U.S. Patent Publication, US 2005/0165316 A1 (2005).
20. E. Haak, T. Haak, Y. Grozinger, G. Krebs, K. H. Usadel, and K. Kusterer, "The impact of contralateral cooling on skin capillary blood cell velocity in patients with diabetes mellitus," *J. Vasc. Res.* **35**, 245–249 (1998).
21. J. E. Tooke, J. Ostergren, P.-E. Lins, and B. Fagrell, "Skin microvascular blood flow control in long duration diabetics with and without complication," *Diabetes Res.* **5**, 189–192 (1987).
22. R. G. Sibbald, S. J. Landolt, and D. Toth, "Skin and diabetes," *Endocrinol. Metab. Clin. North Am.* **25**, 463–472 (1996).
23. V. J. James, L. Belbridge, S. V. McLennan, and D. K. Yue, "Use of x-ray diffraction in study of human diabetic and aging collagen," *Diabetes* **40**, 391–394 (1991).